$$f(\Lambda) = \sin^{-1}\left(\frac{K - K_0}{A}\right)$$

$$K_0 = \frac{1}{2}(K_{\max} - K_{\min}), \qquad A = \frac{1}{2}(K_{\max} - K_{\min}) \tag{11}$$

$$f(\Lambda) = a + b\Lambda + c\Lambda^2 =$$

$$0.32279550 + 0.10489340\Lambda - 0.000074444753\Lambda^2 \tag{12}$$

$$f(\Lambda) = a + b\Lambda + c\Lambda^2 =$$

$$0.32599640 + 0.10469083\Lambda - 0.00012134730\Lambda^2 \tag{13}$$

References

[1]White, F. M., *Viscous Fluid Flows,* McGraw-Hill, New York, 1974.

Euler Solutions for Delta Wings

Andrew B. Wardlaw Jr.* and Stephen F. Davis†
Naval Surface Warfare Center, Silver Spring, Maryland

Nomenclature

b = wing semispan
c = speed of sound
M = Mach number
M_c = Mach number of velocity component normal to ray from wing apex
M_s = Mach number of velocity component normal to upstream side of shock
p = pressure
S_s = (shock spanwise location)/b
s = entropy, $\ell n(p/p_\infty) - \gamma \ell n(\rho/\rho_\infty)$
α = angle of attack
Λ = wing sweep angle measured from normal to wing centerline
ρ = density
$\Sigma\Gamma_z$ = (z component of total crossflow plane circulation)/bc_∞

Subscript
∞ = freestream conditions

Introduction

Miller and Wood[1] have classified the experimentally observed flowfields occurring on delta wings into six different regimes as shown in Fig. 1. These regimes can be divided into three types of flow structures; those which are dominated by a strong leeside vortex, indicated by the dotted region in Fig. 1, those which feature a strong crossflow shock and the remaining regime which exhibits a separation bubble at the wing tip. Euler solutions for delta wings have been extensively studied and a review of this work is provided in Ref. 2. These solutions exhibit two types of structures; separated solutions which feature a large leeside vortex and attached solutions which are dominated by a leeside crossflow shock. Separated solutions are adequate engineering tools for predicting lift, surface pressure, and total pressure loss of the vortex dominated flows illustrated by the dotted regions in Fig. 1. However, the conditions under which computation yields a separated solution have not been systematically studied, and it is not clear that the domain of the computed separated solution coincides with the dotted area in Fig. 1. In fact, numerical experiments using wings of varying thickness, different meshes, varying levels of artificial viscosity and upwind as opposed to centrally differenced schemes show conflicting solution types for the same problem.[3-5] The purpose of this Note is to examine the conditions under which the separated solutions form, trace the evolution of the separated solution, and study the numerical factors which influence inviscid solution type.

Numerical Results

The flow over a delta wing is calculated by solving the steady Euler equations using a Godunov type scheme. The solution is obtained by marching along the delta wing centerline, starting from a uniform axial flow. This marching procedure is only valid for flowfields in which the axial component of velocity remains supersonic everywhere. On a conical body, the solution converges to a conically similar flow. Three variations of the Godunov method have been used. The complete Godunov scheme is a second-order Godunov scheme based on the complete Riemann problem. The approximate Godunov scheme is a second-order scheme which replaces the complete problem with an approximate one. The first-order Godunov scheme is based on the complete Riemann problem. Calculations have been completed using an elliptic, body-fitted coordinate system and a fitted bow shock. Details of the numerical scheme are provided in Ref. 6, and a more extensive description of the numerical results is provided in Ref. 7.

Domain of Attached and Detached Flow

The influence of Mach number and incidence on the occurrence of attached and separated flow is explored in Fig. 1 for zero-thickness wings. A boundary dividing the attached and separated solutions for the complete Godunov scheme is

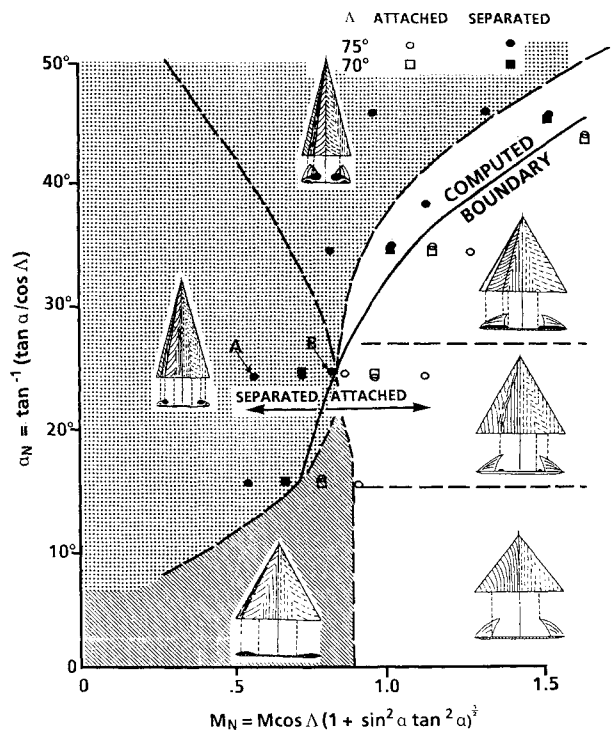

Fig. 1 Computed and measured flowfield type on a delta wing.

Received Dec. 4, 1989. This paper is declared a work of the U.S. Government and is not subject to copyright protection in the United States.

*Aerospace Engineer, Information and Mathematical Sciences Branch. Associate Fellow AIAA.
†Mathematician, Information and Mathematical Sciences Branch.

shown. The specific calculations used to construct this boundary are indicated by the symbols in this figure. This boundary has been computed using a 24 × 72 mesh and delta wings with $\Lambda = 70$ deg and 75 deg and is sensitive to mesh size and scheme type. For example, at $\alpha_n = 25$ deg on a $\Lambda = 75$-deg wing, this boundary is located at $M_N = 0.83$ for a complete Godunov solution on a 24 × 72 mesh. Refining the mesh to 48 × 144 changes the transitional M_N of 0.80, while using the approximate Godunov solver with a 24 × 72 produces a transitional M_N of 0.75. for $\alpha_n > 22$ deg, this boundary approximates the experimentally observed transition between the vortex dominated and shock dominated flow structures. At lower incidences these regimes are separated by the regime featuring a separation bubble at the wing tip. An attached solution with a crossflow shock is calculated for much of this region, even though $M_N < 1$. This shock is a result of a strong expansion which occurs about the wing tip yielding $M_c > 1$ on the leeside of the wing near the tip.

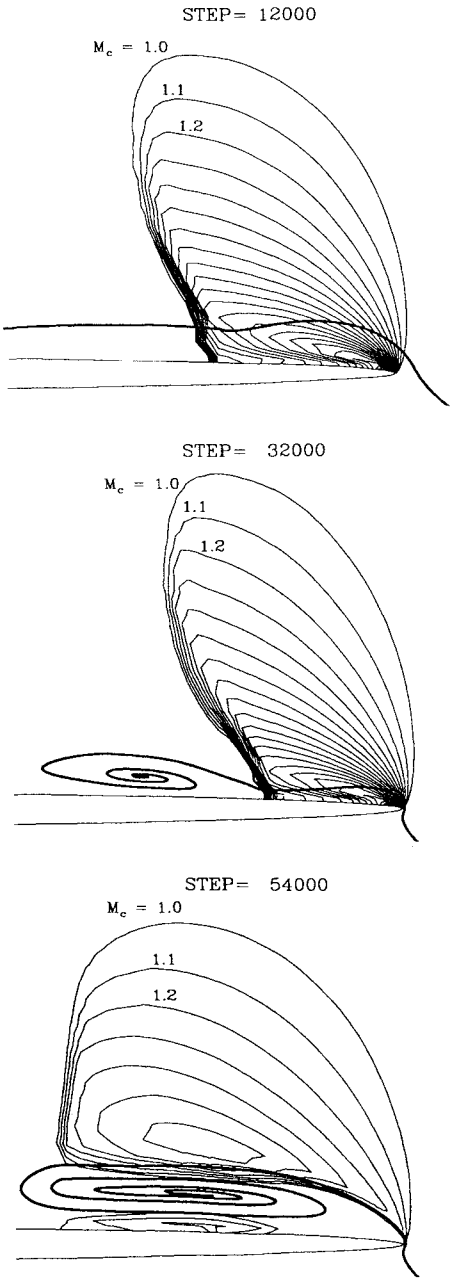

Fig. 2 Flowfield evolution on a 48:1 elliptic delta wing, $M = 2.68$, $\alpha = 6.88$ deg, 48 × 144 mesh; —— Mach contour, ▬▬ streamline.

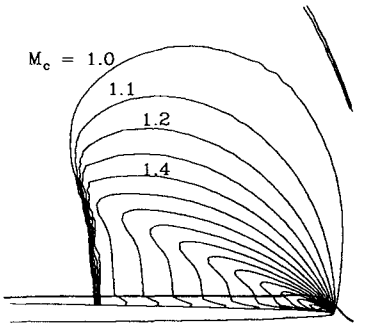

Fig. 3 Crossflow Mach number contours and streamlines on a 48:1 elliptic delta wing, $M = 4.4$, $\alpha = 6.88$ deg, 48 × 44 mesh; —— Mach contour, ▬▬ streamline.

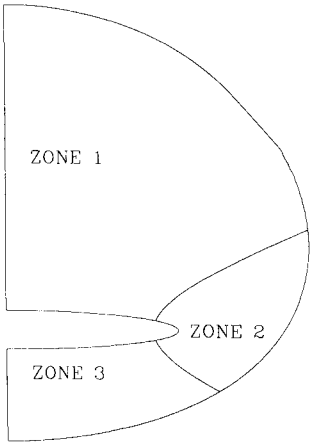

Fig. 4 Computational zone structure.

Flowfield Evolution

The evolution of a separated flowfield on a 48:1 elliptic delta wing, $\Lambda = 75$ deg, at $M = 2.68$ and $\alpha = 6.88$ deg is traced in Fig. 2. Early in the calculation a crossflow shock forms on the lee surface of the wing near the tip. As the computation progresses, this shock moves inboard to a temporary equilibrium position, step 12,000. A vortex forms behind the shock creating a separated flow region which pushes the crossflow shock outboard toward the wing tip, step 32,000. As the crossflow shock moves outboard, its length decreases, and at the wing tip it collapses into a singular point. This leaves a leeside flowfield containing a large vortex, step 54,000. A weak shock is visible above and inboard of the vortex. The singular point features peak surface entropy and vorticity levels, and is the location at which the crossflow velocity reverses.

Repetition of the calculation of the elliptic wing shown in Fig. 2 at $M = 4.4$ leads to an attached solution, as is illustrated in Fig. 3. The evolution of this flowfield parallels the initial development of the separated case. A crossflow shock forms near the leeside wing tip and moves inboard to an equilibrium position. However, a strong vortex does not form downstream of the shock. This prevents the crossflow shock from being displaced to the wing tip, and precludes formation of the separated solution. The absence of a strong vortex can be traced to the weak crossflow shock, with $M_s = 1.4$. By contrast, the separated solution of Fig. 1, step 12,000, has a maximum M_s of 2.1. This stronger shock generates greater circulation which leads to a large vortex, and the separated flowfield.

The separated solution forms later in a calculation as the boundary in Fig. 1 is approached from the left. For example, on a 24 × 72 mesh, case A and B of this figure separate in 400 and 24,000 steps, respectively. When the separation occurs early in a calculation, the shock-vortex interaction is located in a very small region near the wing tip and is difficult to detect.

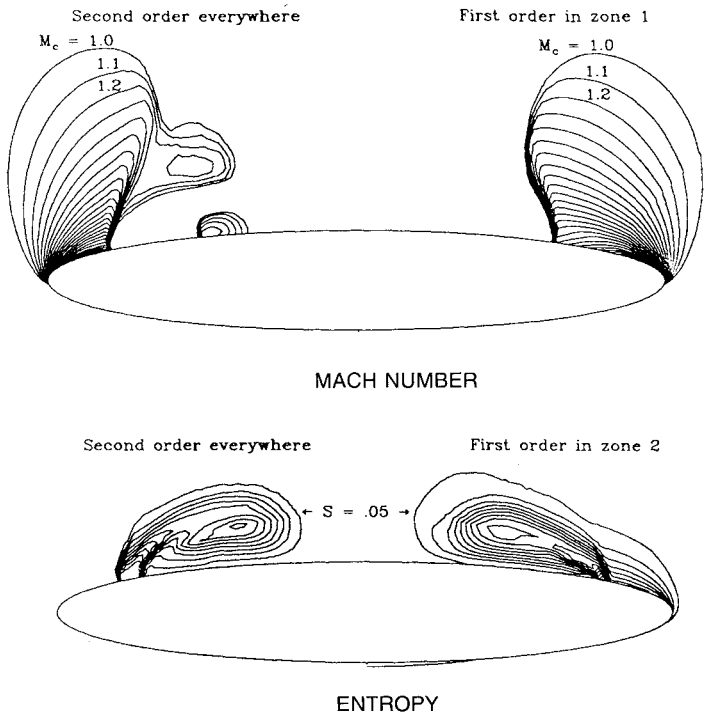

Fig. 5 Influence of accuracy on the solution of a 6:1 elliptic delta wing, $M = 2.68$, $\alpha = 6.88$ deg.

Table 1 Flowfield circulation and shock location vs scheme accuracy on a 6:1 elliptic delta wing, $\Lambda = 15$ deg, at $M = 2.68$ and $\alpha = 15$ deg

Run	Scheme	Zone 1	Zone 2	Zone 3	$\Sigma\Gamma_z$
1	Complete	2nd	2nd	2nd	1.197
2	Complete	1st	2nd	2nd	0.757
3	Complete	2nd	1st	2nd	1.513
4	Approx.	2nd	2nd	2nd	0.854
5	Approx.	1st	2nd	2nd	0.445
6	Approx.	2nd	1st	2nd	1.142

Solution Accuracy and Vorticity Production

The preceding results indicate that the detached flowfield arises from a shock-vortex interaction, but that the domain of such a calculation type is sensitive to the details of the numerical solution, including mesh size and numerical scheme. These findings are consistent with those of other studies where solution type is observed to change with mesh refinement, artificial viscosity level, and scheme type.[3,4,6] To examine the influence of numerical accuracy on solution type, a 6:1 elliptic delta wing is considered. The tip radius of this wing is large enough to permit the tip region to be resolved, allowing the influence of numerical accuracy in different regions of the flowfield to be assessed. This accuracy study is accomplished by dividing the computational domain into three regions shown in Fig. 4. Zone 1 contains the crossflow shock and leeside vortex, zone 2 surrounds the wing tip, while zone 3 consists of the windward portion of the flowfield. The numerical scheme can be reduced to first order in selected zones. Table 1 lists $\Sigma\Gamma_z$ for a number of different runs using a 48 × 144 mesh and the approximate Godunov and complete Godunov schemes. Almost all of the circulation listed in this table is located within the vortex.

The base line vorticity level is obtained using second-order accuracy everywhere, cases 1 and 4. Decreasing the accuracy in zone 1 to first order, cases 2 and 5, decreases $\Sigma\Gamma_z$, while a similar decrease in zone 2 increases $\Sigma\Gamma_z$, cases 3 and 6. Table 1 also indicates that the shock is located further outboard for larger values of $\Sigma\Gamma_z$ indicating that increased vorticity generation leads to a stronger shock-vortex interaction.

An explanation for the behavior of $\Sigma\Gamma_z$ in Table 1 is provided by Fig. 5. In the second-order everywhere calculation, supersonic contours are visible inboard of the crossflow shock. This indicates the presence of a vortex strong enough to induce supersonic crossflow velocities. Making the calculation first order in zone 1 increases solution dissipation in the neighborhood of the vortex which reduces vortex strength and eliminates regions of supersonic M_c inboard of the crossflow shock. Decreasing solution accuracy in the tip region, zone 2, results in spurious entropy generation near the wing tip, as shown in Fig. 5. These errors are convected to the crossflow shock, changing properties on the outboard side of the shock, thereby increasing vorticity production at the shock.

Influence of Numerical Accuracy on Solution Type

Improved accuracy can increase or decrease vortex strength on smooth shapes. The key consideration is where these changes occur. The same trends can be anticipated for thin wings, but here changes in flowfield circulation may also alter solution type. In particular, changes in accuracy which lead to increased flowfield circulation on smooth shapes should promote separated solutions.

The influence of zone 1 accuracy on solution type for thin wings is examined by performing computations on a zero thickness wing at $M = 2.90$ and $\alpha = 6.88$ deg using a 24 × 72 mesh. These conditions lie close to the dividing line between the attached and separated solutions shown in Fig. 1. The resulting solution is attached if zone 1 is first order, but separated for a fully second-order calculation. These cases parallel cases 1 and 2, or 4 and 5, of Table 1 and consistent results are obtained. The attached solution corresponds to case 2 or 5 which exhibits the lower circulation.

The effect of diminishing solution accuracy in the tip region of a thin delta wing is illustrated by considering wings with varying ellipticity. Reduction in wing thickness decreases wing tip resolution and tip region solution accuracy without significantly altering the mesh or solution accuracy in the vicinity of

Table 2 Solution type on delta wings of varying ellipticity and Λ = 15 deg at M = 2.68 and α = 6.88 deg

Mesh Wing	12:1	24:1	48:1	Zero thickness
12×36	Attached	Attached	Attached	Separated
24×72	Attached	Separated	Separated	Separated
48×144	Attached	Attached	Separated	Separated
96×288	Attached	Attached	Separated	Separated

the crossflow shock and leeside vortex. Table 2 illustrates solution type for these wings at M = 2.68. For each mesh, decreasing the wing thickness results in transition from an attached to a separated solution. These observations are consistent with cases 1 and 3, or 4 and 6, of Table 1. Here increased tip error is seen to increase the flowfield circulation, which in the case of a thin wing, promotes separation.

Concluding Remarks

This study has examined the conditions under which separated and attached Euler wing solutions occur and has traced the evolution of each flowfield type. In addition, a numerical study on the effect of accuracy on the solution type has been concluded. Based on these results the following conclusions can be drawn: 1) Euler solution type is determined by a transient shock-vortex interaction. A separated solution occurs in response to the formation of a strong crossflow shock. 2) The Mach number and incidence range for which attached and separated Euler solutions occur is qualitatively similar to the vortex and crossflow shock dominated regimes observed in experiment. However, the location of the boundary between these two types of solutions is sensitive to numerical scheme and mesh size. 3) Euler solution type is influenced by a balance among the errors committed at different locations in the flowfield, not by error level alone. Decreased accuracy on the leeside of the wing promotes attached solutions, while decreased accuracy near the tip favors separated solutions. The last conclusion bears upon the differences noted in the performance of central and upwind schemes.[5] These methods add a different balance of errors to the tip and lee regions of the flowfield.

Acknowledgments

This work was supported by the NSWC Independent Research Fund and NAVAIR. The project monitor was Dale Hutchins (AIR-932J).

References

[1]Miller, D. S., and Wood, R. M., "Leeside Flows over Delta Wings at Supersonic Speeds," *Journal of Aircraft*, Vol. 21, No. 9, 1984, pp. 680–686.

[2]Newsome, R. W., and Kandil, O. A., "Vortical Flow Aerodynamics—Physical Aspects and Numerical Simulation," AIAA Paper 87-0205, Jan. 1987.

[3]Newsome, R. W., "Euler and Navier Stokes Solutions for Flow over a Conical Delta Wing," *AIAA Journal*, Vol. 24, No. 4, 1986, pp. 552–561.

[4]Kandil, O. S., and Chang, A., "Influence of Numerical Dissipation in Computing Supersonic Vortex-Dominated Flows," AIAA Paper 86-1073, May 1986.

[5]Newsome, R. W., and Thomas, J. L., "Computation of Leading Edge Vortex Flows," Vortex Aerodynamic Conference, NASA Langley Research Center, Hampton, Virginia, Oct. 1985.

[6]Wardlaw, A. B., Jr., and Davis, S. F., "A Second Order Godunov Method for Supersonic Tactical Missiles," Naval Surface Warfare Center TR 86-506, Dec. 1986.

[7]Wardlaw, A. B., Jr., and Davis, S. F., "Euler Solutions for Delta Wings," AIAA Paper 89-3398, Aug. 1989.

Vertex-Based Finite-Volume Solution of the Two-Dimensional Navier-Stokes Equations

Sunil Kumar Chakrabartty*
National Aeronautical Laboratory, Bangalore, India

Introduction

PAST experiences in solving inviscid flows by the Euler equations provide many opportunities for exploring possible Navier-Stokes solvers. The finite-volume spatial discretization with the Runge-Kutta time-stepping scheme developed for the Euler equations has been successfully extended by Swanson and Turkel[1] to the computation of viscous flows. Their formulation for the finite-volume scheme is of the cell-centered type, where the flow quantities are associated with the center of a cell in the computational mesh and the fluxes across the cell boundaries are calculated using arithmetic means of values in the adjacent cells. The main advantage of the finite-volume method is its flexibility of treating arbitrary geometries. The cell-centered scheme loses its accuracy with grid stretching and skewness.[2] The nodal point discretization, where the flow quantities are ascribed to the corners of the cell, can give better accuracy for the highly stretched and skewed grids[2,3] that are necessary for viscous flow computations. The surface boundary conditions can be satisfied exactly at the vertices along the body surface, and the pressure on the wall can be computed directly by this scheme, whereas an extrapolation is necessary if one uses the cell-centered scheme. A nodal point finite-volume space discretization scheme[3,4] has been used here to solve the two-dimensional Reynolds-averaged Navier-Stokes equations with a thin-layer type of approximation and a simple two-layer algebraic[5] eddy viscosity model. In the present work, the efficiency of the Runge-Kutta scheme and the benefit of convergence acceleration techniques have also been utilized. The results obtained for turbulent flow past a NACA 0012 airfoil have been compared with available numerical and experimental results.

Governing Equations and Boundary Conditions

The Navier-Stokes equations representing the conservation laws have been considered here in integral form[1] for its ability to treat flow discontinuities automatically. To complete the set of equations for a compressible fluid, a thermodynamic equation of state, Stokes' hypothesis, and Sutherland's law have been considered along with the constant Prandtl number assumption.[3,4]

For turbulent flows the compressible Reynolds-averaged Navier-Stokes equations exhibit a term by term correspondence with their laminar flow counterparts, except that the stress tensor is augmented by the Reynolds stress tensor and the heat flux vector is augmented by the additional turbulence heat flux. To close the time-averaged equations in turbulent flow, the two-layer algebraic eddy viscosity model of Baldwin and Lomax[5] has been used.

The boundary conditions are that the velocity components must be zero (no slip) at the body surface, and the wall temperature is either prescribed or its normal derivative is zero (adiabatic wall, present case). A continuity condition has been

Received Jan. 28, 1989; revision received Dec. 5, 1989.

*Scientist, Computational and Theoretical Fluid Dynamics Division.